Second Virial Coefficient of Oligo- and Poly(methyl methacrylate)s near the Θ Temperature

Fumiaki Abe, Yoshiyuki Einaga, and Hiromi Yamakawa*

Department of Polymer Chemistry, Kyoto University, Kyoto 606-01, Japan

Received September 6, 1994; Revised Manuscript Received October 22, 1994®

ABSTRACT: The second virial coefficient A_2 was determined from light scattering measurements for atactic oligo- and poly(methyl methacrylate)s (a-PMMA) with the fraction of racemic diads $f_r = 0.79$ in acetonitrile at various temperatures below and above Θ (20.0−55.0 °C) in the range of weight-average molecular weight M_w from 6.13×10^2 to ca. 5.0×10^5. The results show that A_2 of a-PMMA depends appreciably on M_w over the whole range of M_w examined even below Θ, in contrast to the previous and literature results for atactic polystyrene (a-PS), for which A_2 is independent of M_w for $M_w > 5 \times 10^3$ below Θ. It is shown that the present data may be quantitatively explained by the Yamakawa theory that takes account of the effect of chain ends on the basis of the helical wormlike chain, yielding rather reasonable values of the binary-cluster integral β between intermediate identical beads and the effective excess binary-cluster integrals β_1 and β_2 associated with the chain end beads. It is found that, as in the case of a-PS, the results for the part $A_2^{(HW)}$ of A_2 without the effect of chain ends are consistent with the two-parameter theory prediction below Θ, giving a single-composite curve irrespective of M_w and temperature when $A_2^{(HW)}M_w^{1/2}$ is plotted against the conventional excluded-volume parameter z. The M_w independence of A_2 below Θ as suggested by Fujita is not generally valid.

Introduction

In a previous paper,[1] we have investigated the molecular-weight M dependence of the second virial coefficient A_2 for atactic oligo- and polystyrenes (a-PS) near the Θ temperature and found that their A_2 depends appreciably on M even below Θ for $M < 5 \times 10^3$, while this dependence almost disappears there for larger M, in agreement with the literature data.[2] It has then been shown that the observed M dependence (or independence) of A_2 near Θ may be quantitatively explained by the recent Yamakawa theory[3,4] of A_2 that takes account of the effect of chain ends on the basis of the helical wormlike (HW) chain.[5,6] From the detailed analysis of the data by this theory, it has also proved that the binary-cluster integral β between intermediate identical beads (or repeat units) is not proportional to $1 - \Theta/T \equiv \tau$ with T the absolute temperature below Θ in contrast to the result above Θ that $\beta \propto \tau$. The inconsistency of the experimental results for A_2 below Θ with the two-parameter theory prediction[7] previously[2,4] claimed may be regarded as arising from both the effect of chain ends and the incorrect assumption of the proportionality of β to τ. It may then be concluded that the M independence of A_2 below Θ for relatively large M is due to an accidental cancellation of the M dependence of $A_2^{(HW)}$ by that of $A_2^{(E)}$, where $A_2^{(E)}$ represents the contribution of the effect of chain ends to A_2 and $A_2^{(HW)}$ is the part of A_2 without this effect. Thus, as previously mentioned,[1] whether A_2 does or does not depend on M below Θ may probably depend on a given polymer−solvent system.

In order to examine this point, in the present work we extend the above study to atactic oligo- and poly(methyl methacrylate)s (a-PMMA), which are remarkably different from a-PS in chain stiffness and local chain conformation.[8−12] Note that it has already been shown[13] that, at the Θ temperature, the M dependence of A_2 for a-PMMA is quite different from that for a-PS and that it may be explained by the Yamakawa theory above. Specifically, in the present work the following points are examined for a-PMMA in acetonitrile: (1) the M dependence (or independence) of A_2 below Θ, (2) the contribution of $A_2^{(E)}$, (3) the proportionality of β to τ, and (4) the validity of the two-parameter theory of $A_2^{(HW)}$ near Θ.

® Abstract published in *Advance ACS Abstracts,* January 1, 1995.

Table 1. Values of M_w, x_w, and M_w/M_n for Atactic Oligo- and Poly(methyl methacrylate)s

sample	M_w	x_w	M_w/M_n
OM6b	6.13×10^2	6.11	1.00
OM8b	8.02×10^2	8.00	1.01
OM12[a]	1.16×10^3	11.6	1.02
OM15[b]	1.50×10^3	15.0	1.03
OM18a	1.83×10^3	18.3	1.05
OM42[a]	4.18×10^3	41.8	1.09
OM76	7.55×10^3	75.5	1.08
MM2a	2.02×10^4	202	1.08
MM5	5.04×10^4	504	1.07
MM31	3.12×10^5	3120	1.08
Mr5	4.82×10^5	4820	1.07

[a] The results for OM12 and OM42 through Mr5 have been reproduced from ref 14 except for those for MM5, which have been reproduced from ref 8. [b] The results for OM15 and OM18a have been reproduced from ref 13.

Experimental Section

Materials. Most of the a-PMMA samples used in this work are the same as those used in the previous studies of the mean-square radii of gyration $\langle S^2\rangle_0$[8] and $\langle S^2\rangle$,[14] the intrinsic viscosities $[\eta]_\Theta$[9] and $[\eta]$,[14] the translational diffusion coefficient D,[12] and A_2,[13] i.e., the fractions separated by preparative gel permeation chromatography (GPC) or fractional precipitation from the original samples prepared by group-transfer polymerization and by radical polymerization. In this work, however, two samples (OM6b and OM8b) were prepared by purification of the previous samples (OM6a and OM8a) with preparative GPC, since the latter samples had been contaminated to some extent in the course of measurements carried out repeatedly in the previous studies. All the samples have a fixed stereochemical composition (the fraction of racemic diads $f_r = 0.79$) independent of molecular weight, possessing hydrogen atoms at both ends of the chain.

The values of the weight-average molecular weight M_w, the weight-average degree of polymerization x_w, and the ratio of M_w to the number-average molecular weight M_n determined by analytical GPC are listed in Table 1. The values of M_w for

0024-9297/95/2228-0694$09.00/0

OM6b and OM8b were determined from light scattering (LS) measurements in acetonitrile at 44.0 °C (Θ). As seen from the values of M_w/M_n, all the samples are sufficiently narrow in molecular weight distribution.

The solvent acetonitrile was purified according to a standard procedure prior to use.

Light Scattering. LS measurements were carried out to determine A_2 (and also M_w) for all the a-PMMA samples in acetonitrile at various temperatures ranging from 20.0 to 55.0 °C. A Fica 50 light-scattering photometer was used for all the measurements with vertically polarized incident light of wavelength 436 nm. For a calibration of the apparatus, the intensity of light scattered from pure benzene was measured at 25.0 °C at a scattering angle of 90°, where the Rayleigh ratio $R_{Uu}(90°)$ of pure benzene was taken as 46.5×10^{-6} cm^{-1}. The depolarization ratio ϱ_u of pure benzene at 25.0 °C was determined to be 0.41 ± 0.01 by the method of Rubingh and Yu.[15]

The conventional method was used for solutions of the samples with $M_w > 10^3$, while the new procedure previously[16] presented was applied to those of the oligomer samples with $M_w < 10^3$ as before[1,13,17] since then the concentration dependences of the density scattering R_d and the optical constant K have significant effects on the determination of A_2 (and also of M_w). In order to determine A_2 by the latter procedure, we measured the reduced total intensity R_{Uv}* of the unpolarized scattered light for vertically polarized incident light, the depolarization ratio ϱ_u, the ratio $\kappa_T/\kappa_{T,0}$ of the isothermal compressibility κ_T of a given solution to that $\kappa_{T,0}$ of the solvent, and the refractive index increment $(\partial\tilde{n}/\partial c)_{T,p}$ at constant T and pressure p for the oligomer solutions and also the first two quantities for the solvent. The values of the refractive index $\tilde{n}$ at finite concentrations c, which were required to calculate K, were calculated with the values of $(\partial\tilde{n}/\partial c)_{T,p}$ for each oligomer sample, as described in the Results section. Measurements of R_{Uv}* were carried out at scattering angles θ ranging from 37.5 to 142.5°, and the mean of the values obtained at different θ was adopted as its value, since it must be independent of θ for oligomers. The values of ϱ_u were obtained by the same method as employed in the calibration of the apparatus.

All the LS data obtained were analyzed by the use of the Berry square-root plot[18] and also the Bawn plot.[19,20] The correction for the anisotropic scattering was then applied to solutions of the samples with $10^3 < M_w \lesssim 4.2 \times 10^3$ (as usual by the use of eq 1 of ref 16).

The most concentrated solution of each sample was prepared by continuous stirring at ca. 50 °C for 1–4 days. It was optically purified by filtration through a Teflon membrane of pore size 0.45 or 0.10 μm. The solutions of lower concentrations were obtained by successive dilution. The polymer mass concentrations c were calculated from the weight fractions with the densities of the solutions. The densities of the solvents and solutions were measured with a pycnometer of the Lipkin–Davison type.

Isothermal Compressibility. Isothermal compressibility measurements were carried out to determine the ratio $\kappa_T/\kappa_{T,0}$ for the oligomer sample OM6b in acetonitrile at 20.0 and 50.0 °C. The apparatus and the method of measurements are the same as those described in the previous paper.[17] It was determined as a function of c and p. The latter was varied from 1 to ca. 50 atm. In this range of p, it was independent of p within experimental error, so that we adopted the mean of the values obtained at various pressures as its value at 1 atm.

Refractive Index Increment. The refractive index increment $(\partial\tilde{n}/\partial c)_{T,p}$ was determined as a function of c and T for each oligomer sample for $M_w < 2 \times 10^3$ at temperatures ranging from 20.0 to 50.0 °C by the use of a Shimadzu differential refractometer.

Results

Light Scattering from Oligo(methyl methacrylate) Solutions. The values of $\kappa_T/\kappa_{T,0}$ obtained for the sample OM6b in acetonitrile are 0.935 and 0.875 at c = 0.1321 and 0.2542 g/cm^3, respectively, at 20.0 °C and 0.918 and 0.870 at c = 0.1272 and 0.2457 g/cm^3, respectively, at 50.0 °C. They coincide with the values previously[13] obtained for the samples OM6a (x_w = 5.94) and OM12 in acetonitrile at 44.0 °C (Θ) within experimental error. Thus the present and previous results may be represented as before by an equation linear in c

$$\kappa_T/\kappa_{T,0} = 1 + kc \tag{1}$$

with $k = -0.500$ cm^3/g for $c \lesssim 0.3$ g/cm^3 irrespective of the values of T and x_w for $293 \lesssim T \lesssim 323$ K and for $6 \leq x_w \leq 12$.

The results for $(\partial\tilde{n}/\partial c)_{T,p}$ at 436 nm for each oligomer sample in acetonitrile are independent of c for $c < 0.20$ g/cm^3 and may be represented by an equation linear in T

$$(\partial\tilde{n}/\partial c)_{T,p} = k_1 + k_2(T - \Theta) \tag{2}$$

where k_2 is independent of x_w and equal to $(3.0 \pm 0.1) \times 10^{-4}$ cm^3/(g K) but k_1 depends on x_w. The values of k_1 determined for the oligomer samples with $6 \lesssim x_w \lesssim 18$ at Θ are given in ref 13 along with the value independent of x_w for the higher-molecular-weight samples. The values of $\tilde{n}$ at finite c may be obtained from eq 2 by integration over c with the values of $\tilde{n}_0$ for the pure solvent acetonitrile at the respective temperatures corresponding to the LS measurements.

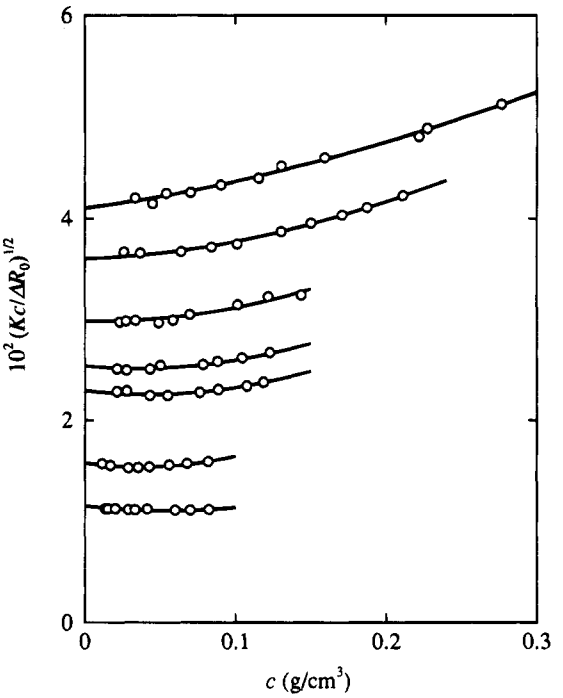

Figure 1. Plots of $(Kc/\Delta R_0)^{1/2}$ against c for a-PMMA in acetonitrile at 25.0 °C. The samples are OM6b, OM8b, OM12, OM15, OM18a, OM42, and OM76 from top to bottom.

Figure 1 shows as examples the Berry square-root plots of the excess Rayleigh ratio ΔR_0 against c for the oligomer samples with $M_w \lesssim 7.55 \times 10^3$ in acetonitrile at 25.0 °C. The data points for each sample follow a curve concave upward, as shown by the solid curve (which represents the values calculated as described below). The results imply that besides the second virial coefficient A_2', the third virial coefficient A_3' at least makes a significant contribution to $Kc/\Delta R_0$ as c is increased, as in the case of a-PS shown in Figure 2 of ref 1. (Here, the prime attached to A_2 and A_3 indicates that they are the *light-scattering* virial coefficients). It

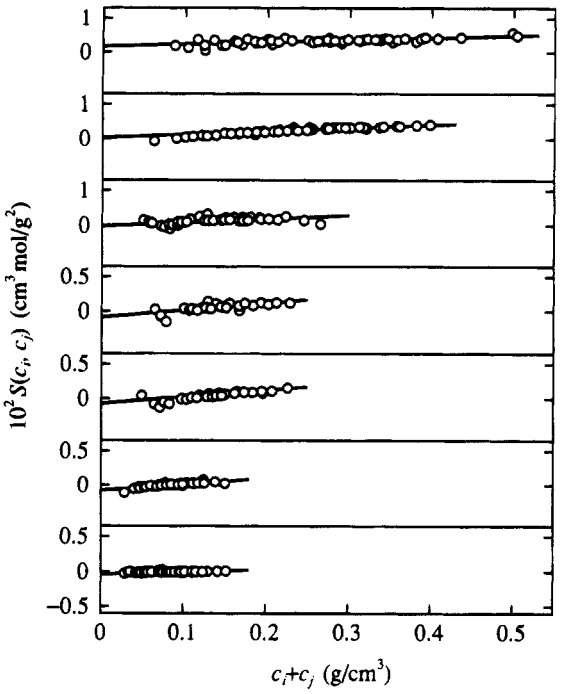

Figure 2. Bawn plots for a-PMMA in acetonitrile at 25.0 °C. The samples are OM6b, OM8b, OM12, OM15, OM18a, OM42, and OM76 from top to bottom.

is then difficult to determine A_2' from the plots with sufficient accuracy.

Therefore, we have made the Bawn plots of these data, as shown in Figure 2, where $S(c_i,c_j)$ is defined by eq 6 of ref 13. As seen from this figure, the data points for each sample follow a straight line, indicating that terms higher than A_3' may be neglected in the range of c studied. From the straight lines indicated, we have determined A_2' and A_3' for each sample in acetonitrile at 25.0 °C. Then we have determined M_w of each sample so that the curve of $(Kc/\Delta R_0)^{1/2}$ calculated with these values of M_w, A_2', and A_3' may give a best fit to the data points in Figure 1. The solid curves in Figure 1 represent the values thus calculated. The good fit of each curve to the corresponding data points indicates that M_w, A_2', and A_3' have been determined with sufficient accuracy.

The data at other temperatures and for the samples with higher molecular weights have been analyzed by the same method. Although the plots are not shown here, the values of M_w, A_2', and A_3' have been determined with an accuracy comparable to or better than the cases of Figures 1 and 2. It has then been proved that the values of A_2' thus obtained may be equated to those of the (osmotic) second virial coefficient A_2 as in the case of the previous results at Θ.[13]

Second Virial Coefficient. The values of A_2 and M_w determined from LS measurements for all the samples in acetonitrile at temperatures ranging from 20.0 to 55.0 °C are summarized in Tables 2 and 3, where in Table 2 some of the results for A_2 previously[13] obtained at 44.0 °C (Θ) are also included and all values of M_w were obtained in the present work. (The present and previous values of M_w of the same sample agree with each other within experimental error.) In Figure 3, the values of A_2 given in Table 2 are plotted against log M_w. It also includes the previous data[13] for the high-molecular-weight samples MM31, Mr5, and Mr8a (M_w = 7.90 × 10^5) at $T > \Theta$ and for MM20 (M_w = 2.07 × 10^5) at Θ. Here the data points at 47.0, 50.0, and 55.0 °C have been shifted upward by 2 × 10^{-4}, 4 × 10^{-4}, and 6 × 10^{-4} cm^3 mol/g^2, respectively, and those at 40.0, 35.0, 30.0, 25.0, and 20.0 °C, downward by 2 × 10^{-4}, 4 × 10^{-4}, 6 × 10^{-4}, 8 × 10^{-4}, and 1 × 10^{-3} cm^3 mol/g^2, respectively. The solid curves connect the data points smoothly.

The overall features of this figure are remarkably different from those for a-PS shown in Figure 5 of ref 1. It is seen that, as M_w is increased, A_2 at 20.0 °C first decreases steeply from positive to negative values, then passes through a minimum, and finally increases gradually to a negative value and that the minimum becomes shallower with increasing T and tends to disappear at $T \gg \Theta$. It is very important to see that A_2 of a-PMMA in acetonitrile depends on M_w over the whole range of M_w examined even below Θ, in contrast to the case of a-PS in cyclohexane, for which A_2 becomes independent of M_w for $M_w > 5 \times 10^3$ and at $T < \Theta$.[1] As stated in the Introduction, it has already been shown in the previous paper[13] that the dependence of A_2 on M_w at Θ may be quantitatively explained by the Yamakawa theory[3,4] that takes account of the effect of chain ends. The appearance of the minimum and the sharp increase in A_2 with decreasing M_w in the range of small M_w at the other temperatures may also be regarded as arising from the same effect.

Discussion

Effects of Chain Ends on A_2. We analyze the data for A_2 in Table 2 by the use of the Yamakawa theory[3,4] that considers the effect of chain ends on the basis of the HW touched-bead model. For convenience, we begin by summarizing the necessary basic equations. The model is such that $n + 1$ beads are arrayed with spacing a between them along the contour of total length $L = na$, where the $n - 1$ intermediate beads are identical and the two end ones are different from the intermediate ones and also from each other in species. Identical excluded-volume interactions are expressed in terms of the conventional binary-cluster integral β, while two kinds of effective excess binary-cluster integrals, β_1 and β_2, are necessary in order to express interactions between unlike beads, β_1 being associated with one end bead and β_2 with two end ones. The HW model itself[5,6] is defined in terms of the three basic model parameters: the constant differential-geometrical curvature κ_0 and torsion τ_0 of its characteristic helix taken at the minimum zero of its elastic energy and the static stiffness parameter λ^{-1}.

According to the theory,[3,4] A_2 in general may be written in the form

$$A_2 = A_2^{(HW)} + A_2^{(E)} \tag{3}$$

where $A_2^{(HW)}$ is that part of A_2 without the effect of chain ends which vanishes at Θ and $A_2^{(E)}$ represents the contribution of this effect to A_2. The first term $A_2^{(HW)}$ may be written as

$$A_2^{(HW)} = (N_A c_\infty^{3/2} L^2 B/2M^2)h \tag{4}$$

where N_A is Avogadro's number, and c_∞ and B are given by

$$c_\infty = \frac{4 + (\lambda^{-1}\tau_0)^2}{4 + (\lambda^{-1}\kappa_0)^2 + (\lambda^{-1}\tau_0)^2} \tag{5}$$

Table 2. Results for A_2 (and M_w) of Atactic Oligo- and Poly(methyl methacrylate)s in Acetonitrile at Various Temperatures

		10^4A_2, cm^3 mol/g^2								
sample	M_w	20.0 °C	25.0 °C	30.0 °C	35.0 °C	40.0 °C	44.0 °C (Θ)	47.0 °C	50.0 °C	55.0 °C
OM6b	613[a]	6.5	8.0	9.5	11.0	12.0	13.0	14.0	15.0	16.5
OM8b	802	0.0	1.5	2.5	4.0	5.0	6.0	6.5	7.0	7.8
OM12	1140	−2.0	−1.0	0.0	1.0	1.8	2.5	3.0	3.7	4.3
OM15	1520	−4.2	−3.5	−2.9	−2.3	−1.9	−1.5[b]	−1.0	−0.50	0.0
OM18a	1870	−4.4	−3.6	−3.0	−2.3	−1.8	−1.4[b]	−0.80	−0.20	0.30
OM42	4200	−4.0	−3.4	−2.8	−2.3	−1.8	−1.3	−0.80	−0.30	0.20
OM76	7550	−2.50	−2.00	−1.80	−1.35	−1.00	−0.68[b]	−0.30	−0.10	0.20
MM2a	20000	−1.37	−1.17	−0.95	−0.69	−0.46	−0.37	−0.15	−0.04	0.12
MM5	50200		−0.92	−0.72	−0.55	−0.32	−0.20[b]	−0.10	0.02	0.15
MM31	314000			−0.52	−0.34	−0.16	−0.02	0.100[b]	0.175[b]	0.256[b]
Mr5	496000			−0.50	−0.34	−0.16	−0.02	0.114[b]	0.184[b]	0.279[b]

[a] All values of M_w were obtained in the present work. [b] Reproduced from ref 13.

and

$$B = \beta/a^2 c_\infty^{3/2} \tag{6}$$

Near Θ (for very small $|z|$), we adopt as the equation for h as before[1,4]

$$h = 1 - 2.865\tilde{z} + 8.851\tilde{z}^2 + 5.077\tilde{z}\tilde{\tilde{z}} - \ldots \tag{7}$$

where the intramolecular and intermolecular scaled excluded-volume parameters $\tilde{z}$ and $\tilde{\tilde{z}}$ are defined by

$$\tilde{z} = (3/4)K(\lambda L)z \tag{8}$$

$$\tilde{\tilde{z}} = [Q(\lambda L)/2.865]z \tag{9}$$

with K and Q being functions only of λL and given by eq 9 of ref 3 and by eq 19 of ref 3 for $\lambda L \gtrsim 1$ (for ordinary flexible polymers), respectively. The conventional excluded-volume parameter z above is now defined by

$$z = (3/2\pi)^{3/2}(\lambda B)(\lambda L)^{1/2} \tag{10}$$

Above Θ ($z > 0$), h is given by eq 18 of ref 3.

Thus, note that h is a function of $\tilde{z}$ and $\tilde{\tilde{z}}$ for $z > 0$ and $z < 0$ and that we may put $h = 1$ approximately for $\lambda L \lesssim 1$. Recall that L is related to M by the equation

$$L = M/M_L \tag{11}$$

with M_L the shift factor as defined as the molecular weight per unit contour length.

The second term $A_2^{(E)}$ in eq 3 may be written in the form

$$A_2^{(E)} = a_1 M^{-1} + a_2 M^{-2} \tag{12}$$

where

$$a_1 = 2N_A\beta_1/M_0$$

$$a_2 = 2N_A\Delta\beta_2 \tag{13}$$

with M_0 the molecular weight of the bead and with

$$\Delta\beta_2 = \beta_2 - 2\beta_1 \tag{14}$$

The parameters β_1 and β_2 are explicitly defined in eqs 22 and ref 3.

Now, in the oligomer region where the relation $h = 1$ holds, $A_2^{(HW)}$ is independent of M, so that we have, from eqs 3 and 12,

$$(A_{2,i} - A_{2,j})/(M_i^{-1} - M_j^{-1}) = a_1 + a_2(M_i^{-1} + M_j^{-1}) \tag{15}$$

with $A_{2,i}$ and $A_{2,j}$ the second virial coefficients for the samples with different molecular weights M_i and M_j, respectively. Equation 15 indicates that a_1 and a_2 may be determined from the intercept and slope of the plot of $(A_{2,i} - A_{2,j})/(M_{w,i}^{-1} - M_{w,j}^{-1})$ vs $M_{w,i}^{-1} + M_{w,j}^{-1}$, respectively. Figures 4 and 5 show such plots for the present data at $T < \Theta$ and at $T \geq \Theta$, respectively, for the low-molecular-weight samples with $M_w \leq 7.55 \times 10^3$, for which h may be equated to unity. We note that the plots at 44.0 °C (Θ) include the data for all the samples given in Table 2 and also for MM20,[13] since $A_2^{(HW)} = 0$ at $T = \Theta$ and then eq 15 holds irrespective of the values of M_w. As was expected, the data points at each temperature can be fitted by a straight line. The results confirm that the appearance of the minimum and the steep increase in A_2 with decreasing M_w for small M_w shown in Figure 3 arise from the effect of chain ends. From the straight lines indicated, we have determined a_1 and a_2 at the respective temperatures. It has then been found that a_2 is independent of T.

Figures 6 and 7 show plots of A_2 against M_w^{-1} with the data corresponding to those in Figures 4 and 5, respectively. From the plots, we have determined $A_2^{(HW)}$ with $h = 1$ at each temperature so that the curve of A_2 as a function of M_w^{-1} calculated from eqs 3 and 12 with these values of $A_2^{(HW)}$ (with $h = 1$), a_1, and a_2 may give a best fit to the data points. The solid curves in Figures 6 and 7 represent the values thus calculated. The good agreement between the calculated and observed values again indicates that the dependence of A_2 on M_w for small M_w arises from the effect of chain ends. Note that the intercept of each solid curve is equal to $A_2^{(HW)}$ with $h = 1$, i.e., the prefactor $(N_A c_\infty^{3/2} L^2 B/2M^2)$, from which we have determined B at the corresponding temperature.

Temperature Dependence of Binary-Cluster Integrals. With the values of B, a_1, and a_2 obtained in the last subsection, we have calculated β, β_1, and β_2 at the respective temperatures from eqs 6 and 13 with eq 14 by taking the repeat unit of the chain as a single bead ($M_0 = 100$). For the calculation of β, we have used the values of the HW model parameters previously[8] determined from $\langle S^2\rangle_0$, i.e., $\lambda^{-1}\kappa_0 = 4.0$, $\lambda^{-1}\tau_0 = 1.1$, $\lambda^{-1} = 57.9$ Å, and $M_L = 36.3$ Å^{-1}.

The values of β (in Å^3) obtained at various temperatures above and below Θ are represented by the unfilled circles in Figure 8. It also includes the values determined by the same method for a-PS in cyclohexane (filled circles) for comparison. It is seen that the T

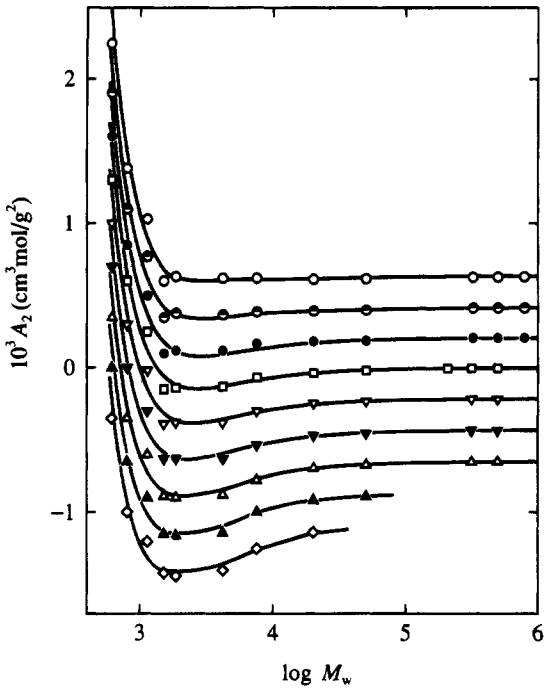

Figure 3. Plots of A_2 against log M_w for a-PMMA in acetonitrile: (○) at 55.0 °C; (◓) at 50.0 °C; (●) at 47.0 °C; (□) at 44.0 °C (⊖); (▽) at 40.0 °C; (▼) at 35.0 °C; (△) at 30.0 °C; (▲) at 25.0 °C; (◇) at 20.0 °C. The data points at 55.0, 50.0, and 47.0 °C are shifted upward by 6×10^{-4}, 4×10^{-4}, and 2×10^{-4} cm^3 mol/g^2, respectively, and those at 40.0, 35.0, 30.0, 25.0, and 20.0 °C, downward by 2×10^{-4}, 4×10^{-4}, 6×10^{-4}, 8×10^{-4}, and 1×10^{-3} cm^3 mol/g^2, respectively. The solid curves connect the data points smoothly.

Table 3. Supplementary Results for A_2 of Atactic Poly(methyl methacrylate) in Acetonitrile at Some Other Temperatures

	$10^4 A_2$, cm^3 mol/g^2					
sample	28.0 °C	33.0 °C	36.0 °C	38.0 °C	41.0 °C	42.0 °C
MM2a	−1.00	−0.75		−0.53		−0.40
MM5	−0.80	−0.60		−0.40		−0.28
MM31	−0.58	−0.40		−0.25		−0.10
Mr5		−0.40	−0.30	−0.24	−0.08	−0.06

dependence of β for a-PMMA in acetonitrile is small compared to that for a-PS in cyclohexane. Then the former β may be well approximated by an empirical equation as a function of τ as follows:

$$\beta = 35\tau \tag{16}$$

The solid straight line in Figure 8 represents the values calculated from this equation.

In Figure 9, the values of β_1 (unfilled circles) and β_2 (filled circles) are plotted against τ. Their absolute values are remarkably larger than the corresponding values for a-PS given in Figure 11 of ref 1. In particular, β_1 for a-PMMA in acetonitrile has large negative values at any τ. However, the results may rather be considered to be of reasonable order of magnitude. The data points for each of β_1 and β_2 follow a straight line as well as for β shown in Figure 8. With these results, for later use, we have also constructed empirical equations for β_1 and β_2 (both in Å^3) as functions of τ as follows:

$$\beta_1 = -65 + 400\tau \tag{17}$$

$$\beta_2 = 700 + 800\tau \tag{18}$$

The solid straight lines for β_1 and β_2 in Figure 9

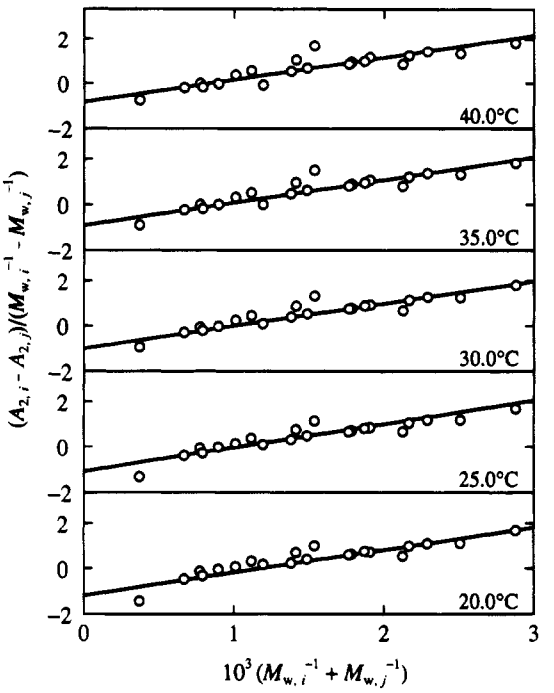

Figure 4. Plots of $(A_{2,i} - A_{2,j})/(M_{w,i}^{-1} - M_{w,j}^{-1})$ against $M_{w,i}^{-1} + M_{w,j}^{-1}$ for a-PMMA in acetonitrile at $T < \Theta$ (see text).

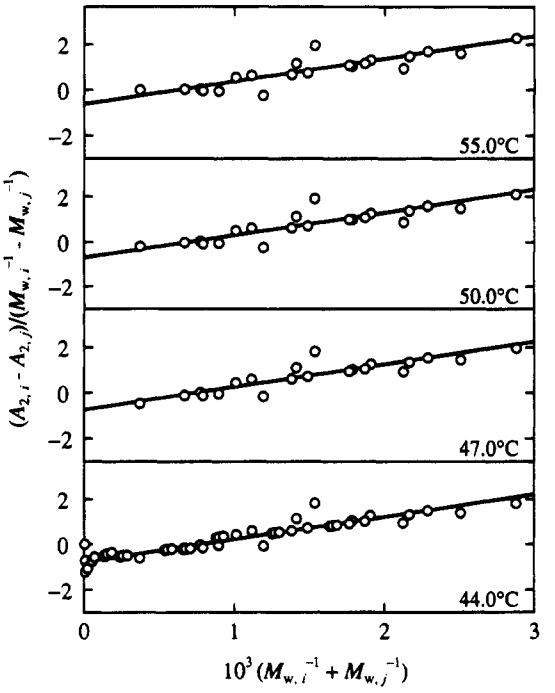

Figure 5. Plots of $(A_{2,i} - A_{2,j})/(M_{w,i}^{-1} - M_{w,j}^{-1})$ against $M_{w,i}^{-1} + M_{w,j}^{-1}$ for a-PMMA in acetonitrile at $T \geq \Theta$ (see text).

represent the values calculated from eqs 17 and 18, respectively.

Dependence of $A_2 M_w^{1/2}$ and $A_2^{(HW)} M_w^{1/2}$ on z. Finally, we consider the quantities $A_2 M_w^{1/2}$ and $A_2^{(HW)} M_w^{1/2}$ as before.[1,4] Figure 10 shows plots of $A_2 M_w^{1/2}$ against z for all the data listed in Tables 2 and 3, where z has been calculated from eq 10 with eqs 6 and 16 and with the values of the HW model parameters given above. The dashed straight line represents the theoretical values calculated from

$$A_2^{(HW)} M^{1/2} = A_2^0 z h \tag{19}$$

with $h = 1$ (the two-parameter theory single-contact

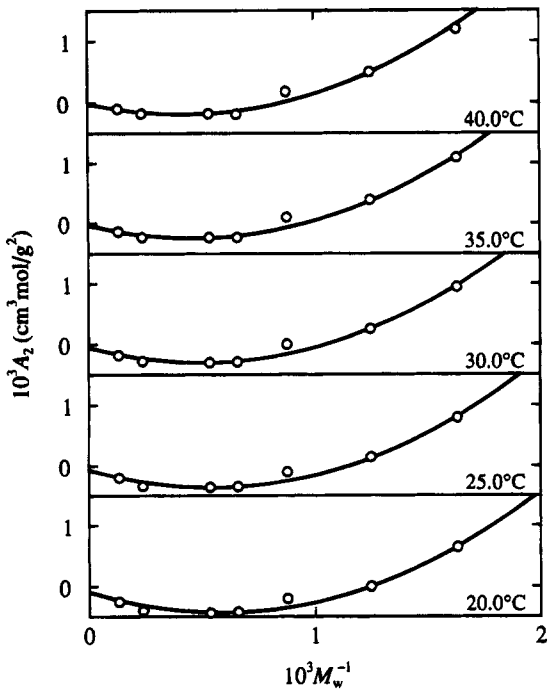

Figure 6. Plots of A_2 against M_w^{-1} for a-PMMA in acetonitrile at $T \leq \Theta$ (see text).

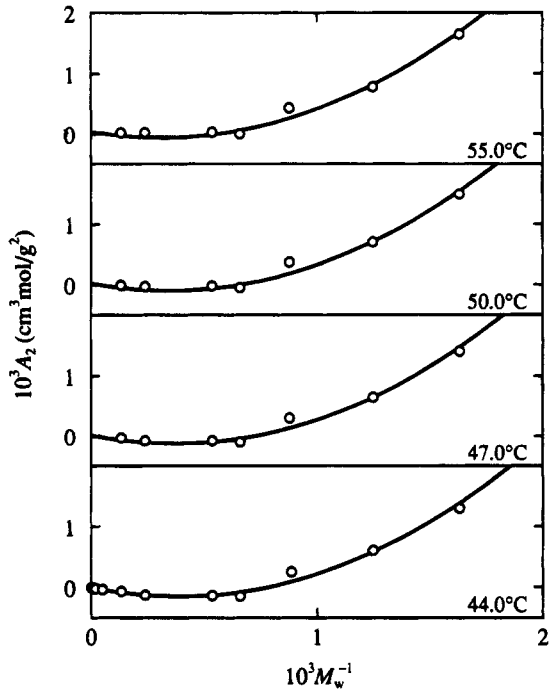

Figure 7. Plots of A_2 against M_w^{-1} for a-PMMA in acetonitrile at $T \geq \Theta$ (see text).

term), assuming that $A_2^{(E)} = 0$, where A_2^0 is given by

$$A_2^0 = 4(\pi/6)^{3/2}N_A(c_\infty/\lambda M_L)^{3/2} \qquad (20)$$

The dotted curve represents the values calculated from eq 19 with the first-order two-parameter perturbation theory of h given by eq 7 with $\tilde{z} = \tilde{\tilde{z}} = z$ (i.e., $h = 1 - 2.865z$). Note that $A_2^0 = 0.224$ cm^3 mol$^{1/2}$/g$^{3/2}$ for a-PMMA.

As was expected, it is seen that the data points cannot form a single-composite curve. Those for the samples OM6b, OM8b, and OM12 are located far above the dashed line with the very large slopes. As M_w is further increased, the data points are first located even below

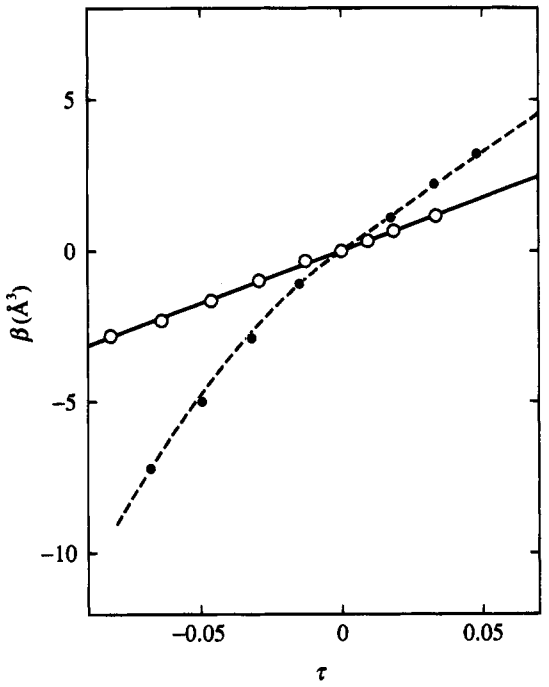

Figure 8. Plots of β against $\tau = 1 - \Theta/T$ for a-PMMA in acetonitrile (○) and a-PS in cyclohexane (●). The solid straight line and the dashed curve represent the values calculated from eq 16 and from eq 20 of ref 1, respectively (see text).

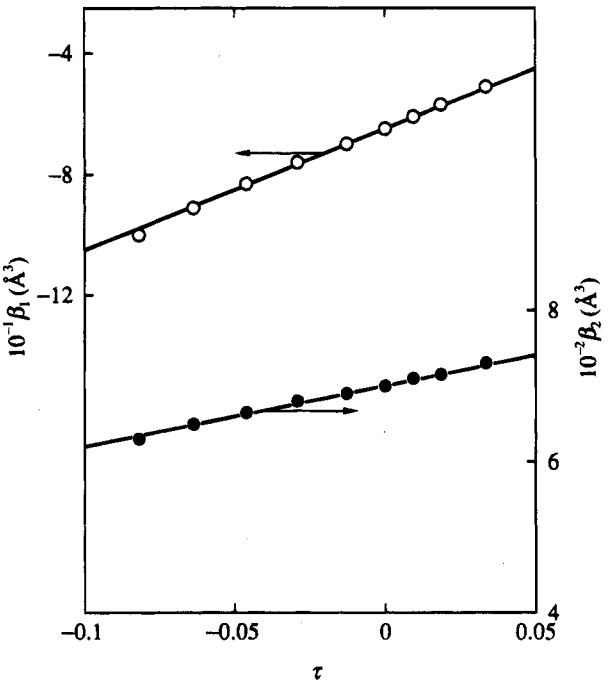

Figure 9. Plots of β_1 and β_2 against τ for a-PMMA in acetonitrile: (○) β_1; (●) β_2. The solid straight lines for β_1 and β_2 represent the values calculated from eqs 17 and 18, respectively.

the dotted curve for $M_w \lesssim 2 \times 10^4$ with the smaller slopes and then between the dashed and dotted lines for higher molecular weights.

Now the results for β_1 and β_2 above allow us to determine the contribution $A_2^{(E)}$ of the effect of chain ends to A_2 from eq 12 with eqs 13, 14, 17, and 18, and therefore the part $A_2^{(HW)}$ of A_2 without this effect by subtraction of $A_2^{(E)}$ from A_2. Figure 11 shows plots of $A_2^{(HW)}M_w^{1/2}$ (divided by A_2^0, for convenience) against the same z as in Figure 10. The dashed and dotted lines have the same meaning as those in Figure 10. It is seen

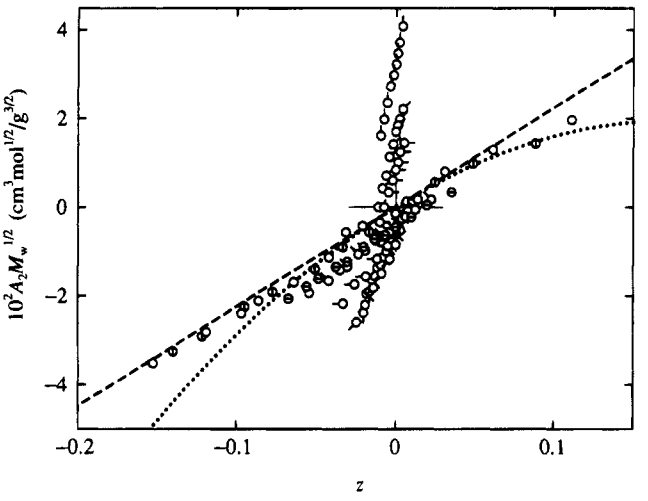

Figure 10. Plots of $A_2M_w^{1/2}$ against z for a-PMMA in acetonitrile: circle with pip up, OM6b; successive 45° clockwise rotations of pips correspond to OM8b, OM12, OM15, OM18a, OM42, OM76, and MM2a, respectively; (⊖) MM5; (⊖) MM31; (○) Mr5. The dashed and dotted curves represent the theoretical values with $A_2^{(E)} = 0$ and $h = 1$ and the first-order two-parameter perturbation theory values, respectively (see text).

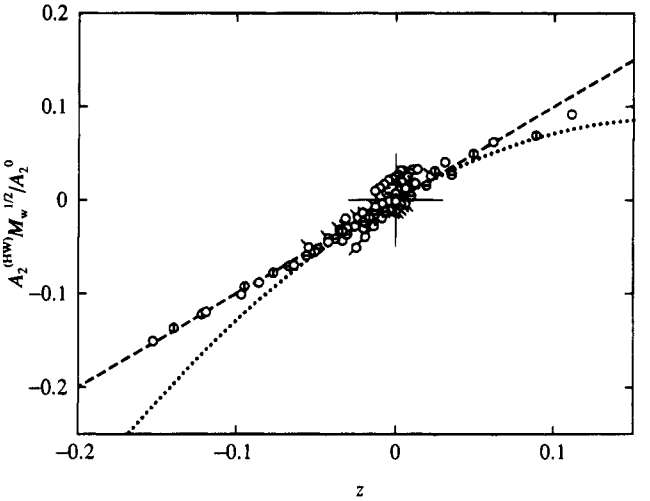

Figure 11. Plots of $A_2^{(HW)}M_w^{1/2}/A_2^0$ against z for a-PMMA in acetonitrile. The symbols and the lines have the same meaning as those in Figure 10.

from Figure 11 that, as in the case of a-PS,[1] all the data points form nearly a single-composite curve (which almost coincides with the corresponding curve for a-PS[1]) within experimental error over a wide range of M_w (from 6.13×10^2 to 4.82×10^5), indicating that the effect of chain stiffness on $A_2^{(HW)}$ and hence A_2 is of little significance below Θ, in contrast to the behavior of A_2 above Θ. More important is the fact that the peculiar deviation of the $A_2M_w^{1/2}$ vs z plot from the two-parameter theory prediction found in Figure 10 disappears in this figure. Thus there is no doubt that the deviation arises from the effect of chain ends.

Conclusion

It has been found that A_2 of a-PMMA below and above Θ depends appreciably on M_w over the whole range of M_w examined ($6.13 \times 10^2 \leq M_w \leq 4.82 \times 10^5$), in contrast to the previous and literature results[1,2] for a-PS, for which the dependence almost disappears below Θ for $M_w > 5 \times 10^3$. The observed dependence of A_2 on M_w may be explained quantitatively by the Yamakawa theory that takes account of the effect of chain ends. The analysis has allowed us to evaluate the contribution $A_2^{(E)}$ of this effect to A_2 at various temperatures to determine the effective excess binary-cluster integrals β_1 and β_2 associated with the chain end beads as functions of temperature T. This has also led to the evaluation of the binary-cluster integral β between intermediate identical beads as a function of T, and therefore of the excluded-volume parameter z. The part $A_2^{(HW)}$ of A_2 without the effect of chain ends obtained as $A_2^{(HW)} = A_2 - A_2^{(E)}$ has been found to be consistent with the two-parameter theory prediction, giving a single-composite curve of $A_2^{(HW)}M_w^{1/2}$ vs z irrespective of the values of M_w and T even below Θ, as in the case of a-PS.

On the other hand, when $A_2M_w^{1/2}$ is plotted against z by the use of the whole A_2 including the effect of chain ends, the plots cannot form a single-composite curve but depend separately also on M_w and T, deviating from the two-parameter-theory prediction. The overall features of the M_w dependence of A_2 are remarkably different from those for a-PS in cyclohexane. The implication is that the way in which the chain ends have an effect on A_2 depends on a given polymer–solvent system. Thus the statement[2,21] that A_2 is independent of M_w below Θ is not generally true.

References and Notes

(1) Yamakawa, H.; Abe, F.; Einaga, Y. *Macromolecules* **1994**, *27*, 5704.
(2) Tong, Z.; Ohashi, S.; Einaga, Y.; Fujita, H. *Polym. J.* **1983**, *15*, 835.
(3) Yamakawa, H. *Macromolecules* **1992**, *25*, 1912.
(4) Yamakawa, H. *Macromolecules* **1993**, *26*, 5061.
(5) Yamakawa, H. *Annu. Rev. Phys. Chem.* **1984**, *35*, 23.
(6) Yamakawa, H. In *Molecular Conformation and Dynamics of Macromolecules in Condensed Systems*; Nagasawa, M., Ed.; Elsevier: Amsterdam, 1988; p 21.
(7) Yamakawa, H. *Modern Theory of Polymer Solutions*; Harper & Row: New York, 1971.
(8) Tamai, Y.; Konishi, T.; Einaga, Y.; Fujii, M.; Yamakawa, H. *Macromolecules* **1990**, *23*, 4067.
(9) Fujii, Y.; Tamai, Y.; Konishi, T.; Yamakawa, H. *Macromolecules* **1991**, *24*, 1608.
(10) Takaeda, Y.; Yoshizaki, T.; Yamakawa, H. *Macromolecules* **1993**, *26*, 3742.
(11) Yoshizaki, T.; Hayashi, H.; Yamakawa, H. *Macromolecules* **1993**, *26*, 4037.
(12) Dehara, K.; Yoshizaki, T.; Yamakawa, H. *Macromolecules* **1993**, *26*, 5137.
(13) Abe, F.; Einaga, Y.; Yamakawa, H. *Macromolecules* **1994**, *27*, 3262.
(14) Abe, F.; Horita, K.; Einaga, Y.; Yamakawa, H. *Macromolecules* **1994**, *27*, 725.
(15) Rubingh, D. N.; Yu, H. *Macromolecules* **1976**, *9*, 681.
(16) Einaga, Y.; Abe, F.; Yamakawa, H. *J. Phys. Chem.* **1992**, *96*, 3948.
(17) Einaga, Y.; Abe, F.; Yamakawa, H. *Macromolecules* **1993**, *26*, 6243.
(18) Berry, G. C. *J. Chem. Phys.* **1966**, *44*, 4550.
(19) Bawn, C. E. H.; Freeman, R. F. J.; Kamalidin, A. R. *Trans. Faraday Soc.* **1950**, *46*, 862.
(20) Norisuye, T.; Fujita, H. *ChemTracts—Macromol. Chem.* **1991**, *2*, 293.
(21) Fujita, H. *Polymer Solutions*; Elsevier: Amsterdam, 1990.

MA941089U